

Article

Enhanced Treatment of Basic Red 46 by Ozonation in a Rotating Packed Bed with Liquid Detention

Peng Xu ¹, Tianyang Wu ¹, Yang Xiang ¹, Jimmy Yun ^{2,3} and Lei Shao ^{1,*} 

¹ Research Center of the Ministry of Education for High Gravity Engineering and Technology, Beijing University of Chemical Technology, Beijing 100029, China; 2021200065@buct.edu.cn (P.X.); 2020200061@mail.buct.edu.cn (T.W.); xiangy@mail.buct.edu.cn (Y.X.)

² School of Chemical Engineering, The University of New South Wales, Sydney, NSW 2052, Australia; jimmy.yun@unsw.edu.au

³ College of Chemical and Pharmaceutical Engineering, Hebei University of Science and Technology, Shijiazhuang 050018, China

* Correspondence: shaol@mail.buct.edu.cn; Tel.: +86-10-6442-1706

Abstract: This study investigated the use of ozone in a rotating packed bed (RPB) with liquid detention for the treatment of Basic Red 46 (BR-46). Liquid detention means that liquid accumulates at the lower section to a certain level in the RPB, which leads to longer liquid residence time and greater liquid holdup in the packing and cavity in the RPB. The experimental results showed that the presence of liquid detention in the RPB significantly enhanced the BR-46 treatment effect and ozone absorption rate. With 200 mL of liquid detention in the RPB, the decolorization rate, COD degradation rate, and ozone absorption rate were 34.7%, 62.8%, and 80.0% higher than those without liquid detention. The effects of the rotational speed of the RPB, ozone concentration, initial BR-46 concentration, liquid and gas flow rates on BR-46 degradation were also investigated, and it was found that the high-gravity environment is beneficial to the degradation of BR-46. These results suggest that with the utilization of the liquid detention phenomena in the high-gravity devices, the applications of the high-gravity technology can be extended to the processes where a long liquid residence time is required.

Keywords: liquid detention; Basic Red 46; ozonation; rotating packed bed; degradation



Citation: Xu, P.; Wu, T.; Xiang, Y.; Yun, J.; Shao, L. Enhanced Treatment of Basic Red 46 by Ozonation in a Rotating Packed Bed with Liquid Detention. *Processes* **2023**, *11*, 1345. <https://doi.org/10.3390/pr11051345>

Academic Editor: Monika Wawrzekiewicz

Received: 30 March 2023

Revised: 20 April 2023

Accepted: 25 April 2023

Published: 26 April 2023



Copyright: © 2023 by the authors. Licensee MDPI, Basel, Switzerland. This article is an open access article distributed under the terms and conditions of the Creative Commons Attribution (CC BY) license (<https://creativecommons.org/licenses/by/4.0/>).

1. Introduction

Azo dyes are the largest category of commercial synthetic dyes, accounting for 70% of the total number of textile dyes. They are extensively used in the food, pharmaceutical, paper, cosmetic, textile, and leather industries due to their wide range of colors and structures [1]. Azo dyes are organic compounds that have one or more azo bonds ($-N=N-$) in a molecule [2]. However, they have been reported to have adverse effects on ecosystems and human health and are present in aqueous environments, sediments, soils, and drinking water supplies [3]. Basic Red 46 (BR-46) is a cationic azo dye that is widely used in coloring nylon, acrylic, and wool fabrics. It is known to be difficult to degrade BR-46 through chemical oxidation, photocatalysis, and biodegradation [4]. Compared to anionic dyes, cationic dyes are more toxic and can enter cells easily by reacting with negatively charged surfaces of cell membranes and gathering in the cytoplasm [5]. Therefore, the removal of these dyes prior to discharge in wastewater has become an important issue.

Advanced oxidation processes (AOPs) based on highly reactive radicals have been shown to be robust technologies for treating organic contaminants in wastewater, providing nearly total degradation [6]. Ozone is a powerful oxidizer with a high oxidation potential of 2.07 V, which directly participates in the reaction with organic matters under acidic conditions (direct oxidation), while alkaline conditions are conducive to forming $\bullet OH$ from ozone, and $\bullet OH$ -based oxidation is considered to be an advanced oxidation

process (indirect oxidation) [7,8]. Under acidic conditions, ozone selectively attacks organic matters, while $\bullet\text{OH}$ reacts with organic matters without selectivity under alkaline conditions [9]. The ozonation process is affected by pH, ozone flow rate and initial organic matter concentration [10].

Over the past few decades, AOPs have been demonstrated to enhance the degradation of various organic compounds [11]. Well-known advanced oxidation technologies mainly include $\text{O}_3/\text{H}_2\text{O}_2$, O_3/UV , O_3/US , Fenton, and AOPs based on persulfate [12–16]. It was found that the degradation of dyes by ozone-based AOPs exhibited the benefits of high reactivity, environmental friendliness and easy operation with ubiquitous air sources [17–19]. However, the ozone oxidation process is significantly affected by the ozone–liquid mass transfer rate due to the low solubility of ozone in water. Thus, a reactor with high gas–liquid mass transfer efficiency is needed to improve the ozone oxidation process [20].

The concept of mass transfer intensification using the rotating packed bed (RPB) was first introduced by Ramshaw [21]. In the RPB, high centrifugal acceleration derived from a rotating rotor disperses the liquid into thinner films and smaller droplets, which enhances gas–liquid mass transfer and intrinsically improves fast reaction processes [22]. The RPB is considered as a reactor that can increase the amount of ozone dissolved per unit time and make wastewater treatment more effective [23].

Recently, we found that the liquid detention phenomena in the RPB can significantly enhance the gas–liquid mass transfer. The phenomena are illustrated in Figure 1. When liquid is detained in the RPB, it will accumulate at the bottom and immerse the lower part of the rotor. In addition, some of the detained liquid will be carried by the rotating rotor to the upper part of the rotor and cavity. Thus, both the liquid residence time and liquid holdup in the RPB increase when the liquid is detained. A longer liquid residence time and greater liquid holdup in the RPB can facilitate the process of ozone mass transfer, suggesting that the phenomena can be used to enhance ozone AOPs for the treatment of organic wastewater.

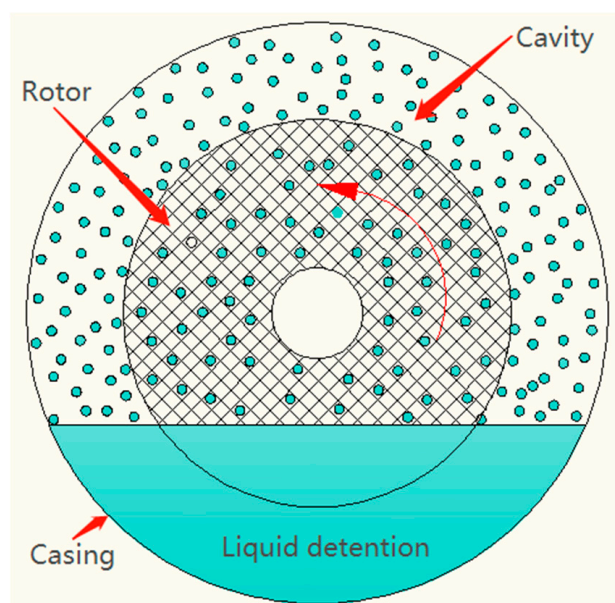


Figure 1. Schematic diagram of liquid detention phenomena in RPB.

Herein, we investigated the effect of liquid detention on ozonation of BR-46 in an RPB for the first time. This work indicates that the RPB with liquid detention enhanced the ozonation efficiency of BR-46 and the absorption rate of ozone, thus providing a novel means for the intensification of organic wastewater treatment by AOPs in high-gravity devices.

2. Materials and Methods

2.1. Materials and Procedure

The experiment used BR-46 (strength: 250%) provided by Shanghai Huayuan Century Trading Co., Shanghai, China. The simulated BR-46 wastewater was prepared by dissolving BR-46 in deionized water. The pH value of the wastewater was measured using a PHSJ-3F pH Meter (Shanghai INESA Scientific Instrument Co., Ltd., Shanghai, China). Table 1 provides the specifications of the RPB.

Table 1. Specifications of the RPB.

Item	Value
Inner diameter of packing	40 mm
Outer diameter of packing	120 mm
Thickness of packing	15 mm
Material of packing	Stainless steel wire mesh
Specific surface area of packing	522 m ² /m ³
Porosity of packing	97%
Inner diameter of casing	180 mm

The experimental setup is presented in Figure 2. Before the experiment, the liquid outlet valve was adjusted to ensure that the inlet and outlet liquid flow rates were equal under the preset experimental conditions. Then, ozone generated from oxygen by a 3S-A10 Ozone Generator (Tonglin High-Tech Technology Co., Ltd., Beijing, China) was introduced into the RPB. Once the ozone concentration at the gas inlet reached the required level, the RPB was turned on before the BR-46 wastewater was pumped into the center of the rotor by a peristaltic pump.

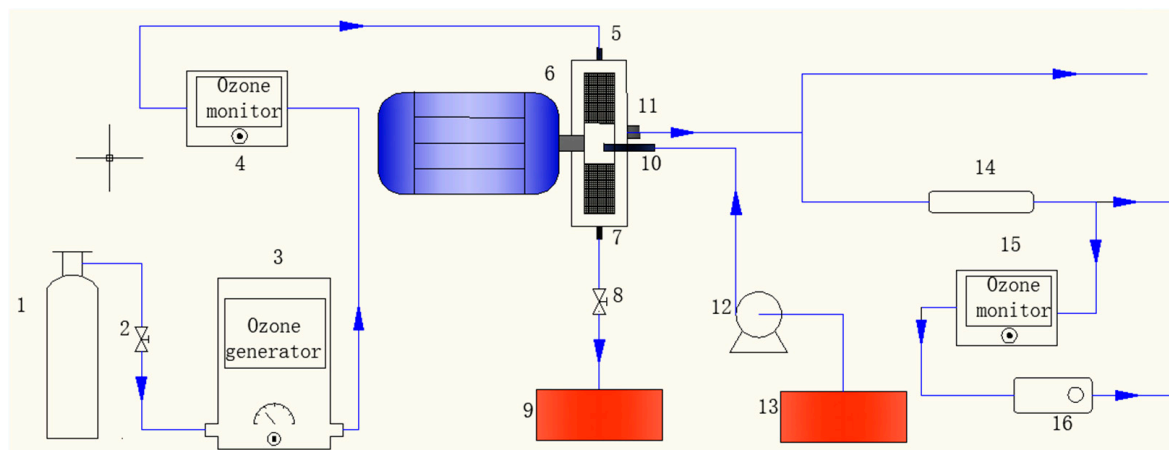


Figure 2. Experimental Setup. (1) Oxygen cylinder; (2) oxygen flowmeter; (3) ozone generator; (4) ozone monitor; (5) gas inlet; (6) RPB; (7) liquid outlet; (8) liquid outlet valve; (9) treated wastewater tank; (10) liquid inlet; (11) gas outlet; (12) pump; (13) original wastewater tank; (14) drying tube; (15) ozone monitor; (16) pump.

When the required amount of liquid was detained in the RPB, the plug of the liquid outlet line was immediately removed to keep the detained liquid in the RPB at a certain level during the experiment. The gas and liquid flows were in counter-current contact in the packing of the RPB, resulting in the absorption of ozone into the liquid stream and degradation of BR-46 by ozone. Finally, the liquid and gas flow exited the RPB through the liquid and gas outlets, respectively. Sampling was conducted from the liquid outlet line when the outlet ozone concentration was stable, and the BR-46 concentration and COD were measured immediately.

2.2. Analytical Methods

The concentration of BR-46 in the wastewater was determined using a DR6000 UV-Vis Spectrophotometer (Hach Corp., Loveland, CO, USA) at a wavelength of 532 nm. The COD in the wastewater was determined using a 5B-6C Multi-parameter Water Quality Analyzer (Lianhua Technology, Beijing, China). The inlet and outlet ozone concentrations were monitored by two detectors (UV300B, Guangzhou Limei Ozone Co., Ltd., Guangzhou, China, and UVOZ-1200, Shandong Zhipu Measurement and Control Technology Co., Ltd., Zibo, China), respectively. The decolorization rate, COD degradation rate, and ozone absorption rate were calculated by the following Equations (1)–(3), respectively:

$$D_B = \frac{C_0 - C_1}{C_0} \times 100\% \quad (1)$$

where D_B represents the decolorization rate of BR-46 wastewater, while C_0 and C_1 represent the initial and final BR-46 concentrations before and after treatment, respectively, (mg/L).

$$R_{\text{COD}} = \frac{\text{COD}_0 - \text{COD}_1}{\text{COD}_0} \times 100\% \quad (2)$$

where R_{COD} represents the COD degradation rate, while COD_0 and COD_1 represent the initial and final COD of the BR-46 wastewater before and after treatment, respectively, (mg/L).

$$A_B = \frac{\omega_0 - \omega_1}{\omega_0} \times 100\% \quad (3)$$

where A_B represents the ozone absorption rate, while ω_0 and ω_1 represent the ozone concentration at the inlet and outlet of RPB, respectively, (mg/L).

3. Results and Discussion

3.1. Effect of Liquid Detention

In the degradation of BR-46 by ozonation, ozone and $\bullet\text{OH}$ first break the $-\text{N}=\text{N}-$ bond of BR-46 to produce various intermediates, which are further attacked by ozone and $\bullet\text{OH}$ to eventually produce N_2 , NO_3^- , CO_2 , H_2O , etc. [24,25].

Figure 3 shows the effect of liquid detention volume (V) on the ozonation of BR-46 in the liquid detention range of 0–300 mL. The results indicate that the presence of liquid detention in the RPB enhances the treatment efficiency of BR-46 and increases the absorption rate of ozone. In the absence of liquid detention in the RPB, the decolorization rate, COD degradation rate, and ozone absorption rate were 61.3%, 18.3%, and 40.1%, respectively. However, with 200 mL of liquid detention, the decolorization rate, COD degradation rate, and ozone absorption rate increased to 82.6%, 29.8%, and 72.2%, respectively, which were 34.7%, 62.8%, and 80.0% higher than those without liquid detention, suggesting that liquid detention in the RPB can significantly enhance the absorption of ozone and the degradation of BR-46.

As shown in Figure 1, liquid detention means that liquid does not flow out of the RPB immediately, but accumulates and stays at the lower section of the RPB for a certain time after it is ejected from the rotor. Thus, the liquid residence time in the RPB greatly extends. Furthermore, some of the detained liquid will be carried by the rotating rotor to the upper part of the rotor, causing an increase in liquid holdup in the packing of the rotor and the cavity of the RPB. The increase in the liquid residence time and holdup is conducive to the absorption of ozone and thus the degradation of BR-46.

However, a further increase in the liquid detention to more than 200 mL resulted in a lower treatment effect, which may be ascribed to the reduced gas flow channel and accelerated gas flow rate as a result of the excessive liquid detention, thereby leading to the decreased ozone absorption rate and reduced treatment effect of BR-46.

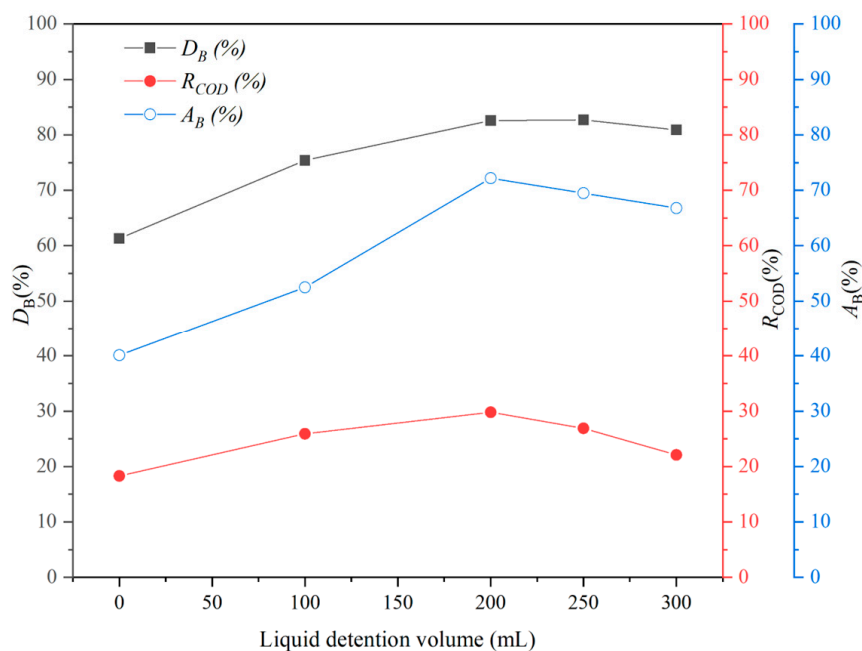


Figure 3. Effect of liquid detention volume on BR-46 degradation. Ozone concentration (C) = 20 mg/L; gas flow rate (G) = 75 L/h; liquid flow rate (L) = 15 L/h; rotational speed (R) = 800 rpm; initial BR-46 concentration (C_{BR-46}) = 300 mg/L.

3.2. Effect of Rotational Speed of RPB

Figure 4 illustrates the impact of the rotational speed of the RPB on the degradation efficiency of BR-46 in the rotational speed range of 200–1000 rpm. With an increase in rotational speed from 200 rpm to 600 rpm, the decolorization rate, COD degradation rate, and ozone absorption rate increased from 78.0%, 28.8%, and 40.1% to 95.3%, 33.7%, and 63.2%, respectively. When the rotational speed exceeded 600 rpm, the decolorization rate, COD degradation rate, and ozone absorption rate remained steady at approximately 95%, 33%, and 63%, respectively.

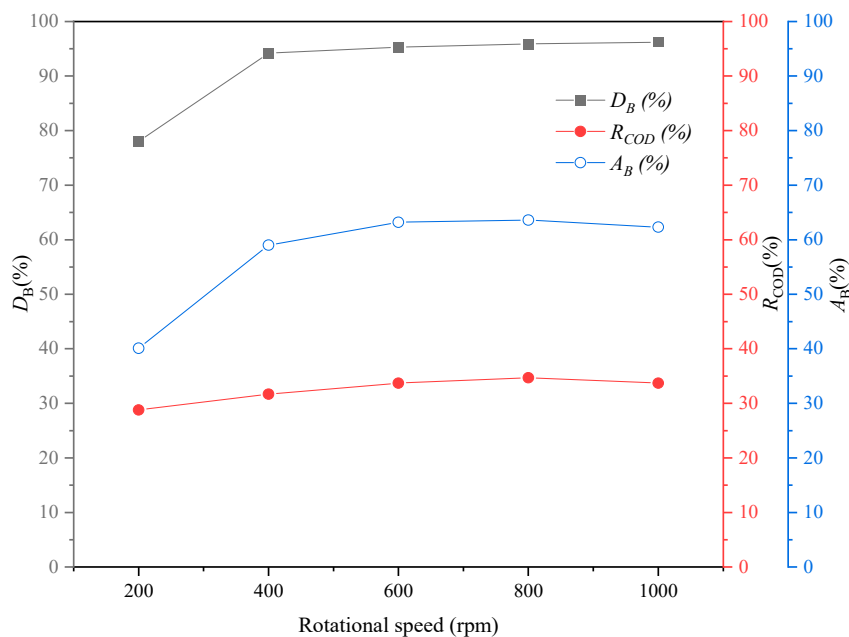


Figure 4. Effect of rotational speed on BR-46 degradation. $V = 200$ mL; $G = 75$ L/h; $L = 15$ L/h; $C = 30$ mg/L; $C_{BR-46} = 300$ mg/L.

The reason behind this is that a higher rotational speed increases the turbulence of the liquid in the RPB, leading to its dispersion into thinner films and smaller droplets, thus increasing the area of gas–liquid mass transfer. As a result, more ozone dissolves in the wastewater, leading to the higher degradation efficiency of BR-46.

However, the liquid residence time in the packing decreases with an increasing rotational speed, which is unfavorable for the degradation of BR-46. When the rotational speed increases over 600 rpm, the unfavorable effect of reduced liquid residence time offsets the favorable effect of increased dispersion of the BR-46 solution, resulting in almost stable ozone absorption rate, decolorization rate, and COD degradation rate. Liu et al. [26] also observed similar phenomena in the inactivation of *E. coli* by ozone in an RPB.

3.3. Effect of Gaseous Ozone Concentration

Figure 5 shows the effect of ozone concentration in a gas stream on the ozonation of BR-46 in the gaseous ozone concentration range of 10–50 mg/L. The results indicate that as the ozone concentration increased from 10 mg/L to 50 mg/L, the decolorization rate and COD degradation rate increased, while the ozone absorption rate decreased. At an ozone concentration of 30 mg/L, the decolorization rate, COD degradation rate, and ozone absorption rate were 97.0%, 29.4%, and 57.7%, respectively. The amount of ozone dissolved in wastewater increases with the increase in gaseous ozone concentration, leading to an increase in the amount of ozone reacting with the wastewater and promoting the degradation of BR-46. However, with the increase in ozone concentration, more ozone entering the RPB is discharged without participating in a reaction, resulting in a decrease in the ozone absorption percentage. Similar phenomena have also been observed by other researchers [27].

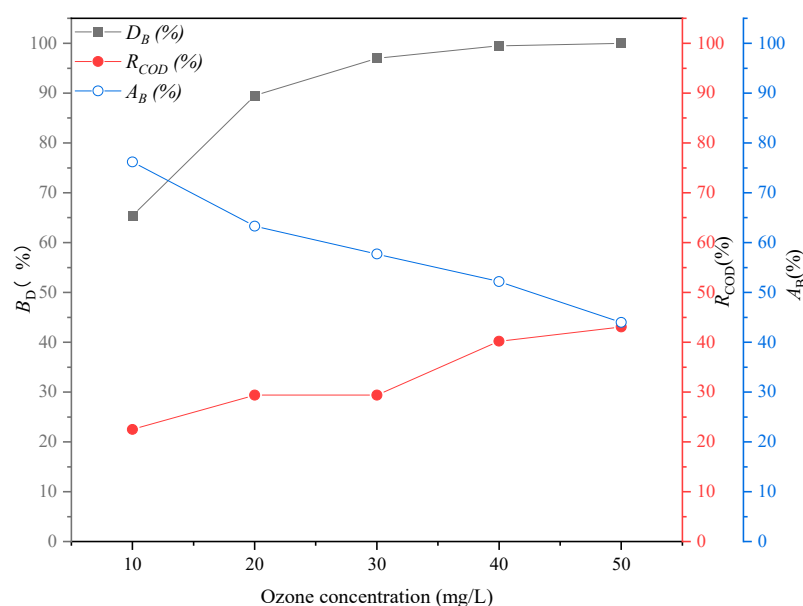


Figure 5. Effect of ozone concentration on BR-46 degradation. $V = 200$ mL; $G = 75$ L/h; $L = 15$ L/h; $R = 800$ rpm; $C_{BR-46} = 300$ mg/L.

3.4. Effect of Initial BR-46 Concentration

Figure 6 shows the effect of the initial BR-46 concentration on the degradation efficiency of BR-46 in the BR-46 concentration and COD range of 92.8–512.0 mg/L and 57.2–255.8 mg/L, respectively. As the initial concentration increased from 100 mg/L to 500 mg/L, the decolorization rate and COD degradation rate decreased from 100% and 50.0% to 85.4% and 27.6%, respectively, while the ozone absorption rate increased from 31.8% to 63.7%. This is because the increase in BR-46 concentration increases the mass transfer driving force and promotes ozone absorption. However, with the constant ozone

concentration, the increase in BR-46 concentration results in the insufficiency of oxidants, leading to the reduction in the degradation efficiency of BR-46. It was found that the degradation of Bisphenol A by ozone in an RPB also followed the same rules [28].

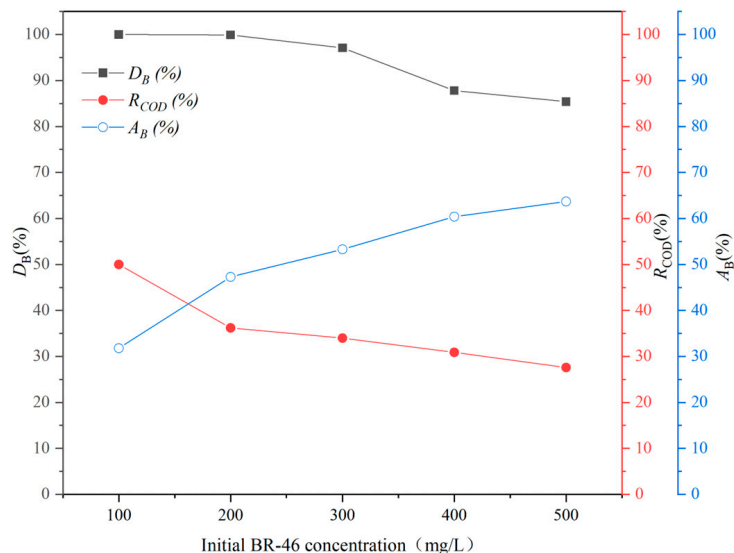


Figure 6. Effect of initial BR-46 concentration on BR-46 degradation. $V = 200$ mL; $G = 75$ L/h; $L = 15$ L/h; $R = 800$ rpm; $C = 30$ mg/L.

3.5. Effect of Liquid Flow Rate

Figure 7 shows the effect of the liquid flow rate on the degradation efficiency of BR-46 in the liquid flow rate range of 5–25 L/h. As the liquid flow rate increased from 5.0 to 25 L/h, the decolorization rate and COD degradation rate decreased from 100% and 44.9% to 80.9% and 28.4%, respectively, while the ozone absorption rate increased from 41.0% to 71.2%. The decrease in the residence time of liquid in the RPB due to the increase in liquid flow rate leads to the discharge of the BR-46 solution with underreaction with ozone, resulting in a decrease in the decolorization rate and COD degradation rate. However, the increase in the gas–liquid interfacial area due to the elevation of the liquid flow rate promotes ozone absorption, leading to an increase in the ozone absorption rate. Similar observations have also been reported for the ozonation of amaranth in a rotating zigzag bed [20].

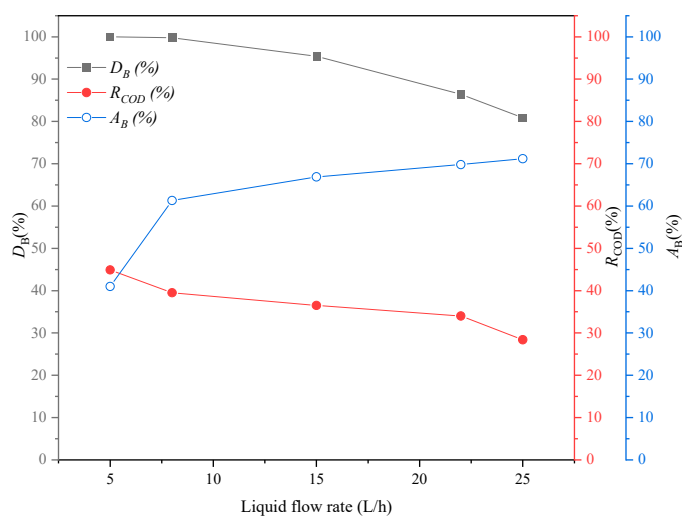


Figure 7. Effect of liquid flow rate on BR-46 degradation. $V = 200$ mL; $G = 75$ L/h; $R = 800$ rpm; $C = 30$ mg/L; $C_{BR-46} = 300$ mg/L.

3.6. Effect of Gas Flow Rate

Figure 8 demonstrates the effect of the gas flow rate on the degradation efficiency of BR-46 in the gas flow rate range of 30–90 L/h. With an increase in the gas flow rate from 30 L/h to 90 L/h, the decolorization rate and COD degradation rate increased from 65.4% and 24.0% to 97.0% and 37.0%, respectively, while the ozone absorption rate decreased from 94.0% to 55.8%.

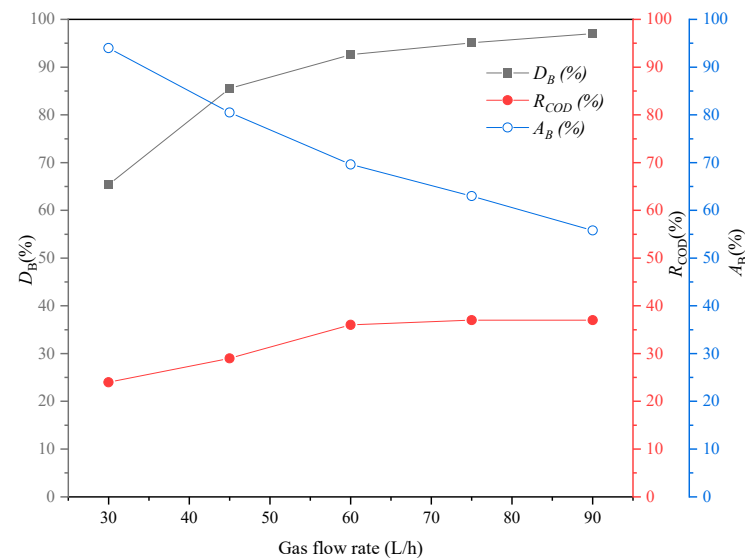


Figure 8. Effect of gas flow rate on BR-46 degradation. $V = 200$ mL; $R = 600$ rpm; $L = 15$ L/h; $C = 30$ mg/L; $C_{BR-46} = 300$ mg/L.

The increase in the gas flow rate leads to an increase in the turbulence of the gas and liquid phases, enabling more ozone to dissolve in the wastewater, thereby increasing the decolorization rate and COD degradation rate. However, a higher gas flow rate leads to a higher flow speed of the ozone gas in the RPB, resulting in shorter gas–liquid contact time and thus a decreased ozone absorption rate. The phenomena agree with the observations of Wang et al. on Bisphenol A ozonation in an RPB [28].

4. Conclusions

This study investigated the ozonation of BR-46 in the RPB with liquid detention under various process conditions. The experimental results showed that the presence of liquid detention in the RPB enhanced the ozone absorption rate and the ozonation of BR-46. With 200 mL of liquid detention, the decolorization rate, COD degradation rate, and ozone absorption rate were 34.7%, 62.8%, and 80.0% higher than those without liquid detention, respectively, suggesting that liquid detention in the RPB can significantly promote ozone absorption and BR-46 degradation. It is deduced that the liquid detention leads to the increase in liquid residence time and holdup in the RPB, which is conducive to the absorption of ozone and thus the degradation of organic matters. It was also found that the decolorization rate, COD degradation rate, and ozone absorption rate increased from 78.0%, 28.8%, and 40.1% to 95.3%, 33.7%, and 63.2%, respectively, with an increase in the rotational speed of the RPB from 200 rpm to 600 rpm. These results indicated that the utilization of the liquid detention phenomena in the high-gravity technology can overcome the shortcomings of insufficient liquid residence time in this technology and extend its applications to kinetics-limited processes.

Author Contributions: Conceptualization, L.S.; methodology, P.X.; validation, T.W.; formal analysis, Y.X.; investigation, P.X.; resources, J.Y.; data curation, T.W.; writing—original draft preparation, P.X.; writing—review and editing, J.Y.; supervision, L.S.; project administration, L.S.; funding acquisition, L.S. All authors have read and agreed to the published version of the manuscript.

Funding: This research was funded by the National Natural Science Foundation of China, grant number 22178021.

Data Availability Statement: Not applicable.

Acknowledgments: The authors gratefully acknowledge the financial support from the National Natural Science Foundation of China (No. 22178021).

Conflicts of Interest: The authors declare no conflict of interest.

References

1. Sen, S.K.; Raut, S.; Bandyopadhyay, P.; Raut, S. Fungal decolouration and degradation of azo dyes: A review. *Fungal Biol. Rev.* **2016**, *30*, 112–133. [[CrossRef](#)]
2. Kong, S.; Zhang, W.; Gao, S.; Chen, D. Immobilized CeO₂ for adsorption of azo dye. *J. Exp. Nanosci.* **2019**, *14*, 107–115. [[CrossRef](#)]
3. Shi, Y.; Yang, Z.; Xing, L.; Zhang, X.; Li, X.; Zhang, D. Recent advances in the biodegradation of azo dyes. *World J. Microb. Biot.* **2021**, *37*, 1–18. [[CrossRef](#)] [[PubMed](#)]
4. Torres-Luna, J.A.; Giraldo-Gómez, G.I.; Sanabria-González, N.R.; Carriazo, J.G. Catalytic degradation of real-textile azo-dyes in aqueous solutions by using Cu–Co/halloysite. *Bull. Mater. Sci.* **2019**, *42*, 137. [[CrossRef](#)]
5. Kapoor, R.T.; Sivamani, S. Adsorptive Potential of Orange Peel Biochar for Removal of Basic Red Dye and Phytotoxicity Analysis. *Chem. Eng. Technol.* **2023**, *46*, 756–765. [[CrossRef](#)]
6. Guo, Y.; Zeng, Z.; Zhu, Y.; Huang, Z.; Cui, Y.; Yang, J. Catalytic oxidation of aqueous organic contaminants by persulfate activated with sulfur-doped hierarchically porous carbon derived from thiophene. *Appl. Catal. B Environ.* **2018**, *220*, 635–644. [[CrossRef](#)]
7. Malik, S.N.; Ghosh, P.C.; Vaidya, A.N.; Mudliar, S.N. Hybrid ozonation process for industrial wastewater treatment: Principles and applications: A review. *J. Water Process Eng.* **2020**, *35*, 101193. [[CrossRef](#)]
8. Toro, C.A.T.; Dagostin, J.L.A.; Vasques, É.C.; Spier, M.R.; Igarashi-Mafra, L.; Dantas, T.L.P. Effectiveness of ozonation and catalytic ozonation (iron oxide) in the degradation of sunset yellow dye. *Can. J. Chem. Eng.* **2020**, *98*, 2530–2544. [[CrossRef](#)]
9. Otieno, B.; Apollo, S.; Kabuba, J.; Naidoo, B.; Simate, G.; Ochieng, A. Ozonolysis pre-treatment of waste activated sludge for solubilization and biodegradability enhancement. *J. Environ. Chem. Eng.* **2019**, *7*, 102945. [[CrossRef](#)]
10. Otieno, B.; Apollo, S.; Kabuba, J.; Naidoo, B.; Ochieng, A. Ozonolysis post-treatment of anaerobically digested distillery wastewater effluent. *Ozone Sci. Eng.* **2019**, *41*, 551–561. [[CrossRef](#)]
11. Dang, T.T.; Do, V.M.; Trinh, V.T. Nano-catalysts in ozone-based advanced oxidation processes for wastewater treatment. *Curr. Pollut. Rep.* **2020**, *6*, 217–229. [[CrossRef](#)]
12. Ouali, S.; Biard, P.F.; Loulergue, P.; You, R.; Nasrallah, N.; Maachi, R.; Szymczyk, A. Water treatment intensification using a monophasic hybrid process coupling nanofiltration and ozone/hydrogen peroxide advanced oxidation. *Chem. Eng. J.* **2022**, *437*, 135263. [[CrossRef](#)]
13. Li, R.; Siriwardena, D.; Speed, D.; Fernando, S.; Holsen, T.M.; Thagard, S.M. Treatment of azole-containing industrial wastewater by the fenton process. *Ind. Eng. Chem. Res.* **2021**, *60*, 9716–9728. [[CrossRef](#)]
14. Tichonovas, M.; Krugly, E.; Jankunaite, D.; Racys, V.; Martuzevicius, D. Ozone-UV-catalysis based advanced oxidation process for wastewater treatment. *Environ. Sci. Pollut. Res.* **2017**, *24*, 17584–17597. [[CrossRef](#)] [[PubMed](#)]
15. Zhang, H.; Zhang, Y.; Qiao, T.; Hu, S.; Liu, J.; Zhu, R.; Yang, K.; Li, S.; Zhang, L. Study on ultrasonic enhanced ozone oxidation of cyanide-containing wastewater. *Sep. Purif. Technol.* **2022**, *303*, 122258. [[CrossRef](#)]
16. Qi, F.; Zeng, Z.; Wen, Q.; Huang, Z. Enhanced organics degradation by three-dimensional (3D) electrochemical activation of persulfate using sulfur-doped carbon particle electrode: The role of thiophene sulfur functional group and specific capacitance. *J. Hazard. Mater.* **2021**, *416*, 125810. [[CrossRef](#)]
17. Wang, J.; Yuan, R.; Feng, Z.; Ma, F.; Zhou, B.; Chen, H. The advanced treatment of textile printing and dyeing wastewater by hydrodynamic cavitation and ozone: Degradation, mechanism, and transformation of dissolved organic matter. *Environ. Res.* **2022**, *215*, 114300. [[CrossRef](#)]
18. Muniyasamy, A.; Sivaporul, G.; Gopinath, A.; Lakshmanan, R.; Altaee, A.; Achary, A.; Chellam, P.V. Process development for the degradation of textile azo dyes (mono-, di-, poly-) by advanced oxidation process-Ozonation: Experimental & partial derivative modelling approach. *J. Environ. Manag.* **2020**, *265*, 110397. [[CrossRef](#)]
19. Parsa, J.B.; Negahdar, S.H. Treatment of wastewater containing Acid Blue 92 dye by advanced ozone-based oxidation methods. *Sep. Purif. Technol.* **2012**, *98*, 315–320. [[CrossRef](#)]
20. Wu, T.; Zhang, H.; Liu, Z.; Liu, T.; Jiang, P.; Arowo, M.; Shao, L. Amaranth wastewater treatment by intensified ozonation in a rotating zigzag bed. *J. Water Process Eng.* **2022**, *49*, 102984. [[CrossRef](#)]
21. Gao, W.; Song, Y.; Jiao, W.; Liu, Y. A catalyst-free and highly efficient approach to ozonation of benzyl alcohol to benzoic acid in a rotating packed bed. *J. Taiwan Inst. Chem. Eng.* **2019**, *103*, 1–6. [[CrossRef](#)]
22. Han, R.; Fang, X.; Song, Y.; Wang, L.; Lu, Y.; Ma, H.; Xiao, H.; Shao, L. Study on the oxidation of ammonium sulfite by ozone in a rotating packed bed. *Chem. Eng. Process.* **2022**, *173*, 108820. [[CrossRef](#)]
23. Yang, P.; Luo, S.; Liu, H.; Jiao, W.; Liu, Y. Aqueous ozone decomposition kinetics in a rotating packed bed. *J. Taiwan Inst. Chem. Eng.* **2019**, *96*, 11–17. [[CrossRef](#)]

24. Karimi-Shamsabadi, M.; Behpour, M. Comparing photocatalytic activity consisting of Sb_2S_3 and Ag_2S on the $\text{TiO}_2\text{-SiO}_2/\text{TiO}_2$ nanotube arrays-support for improved visible-light-induced photocatalytic degradation of a binary mixture of basic blue 41 and basic red 46 dyes. *Int. J. Hydrogen Energy* **2021**, *46*, 26989–27013. [[CrossRef](#)]
25. Berkani, M.; Kadmi, Y.; Bouchareb, M.K.; Bouhelassa, M.; Bouzaza, A. Combination of a Box-Behnken design technique with response surface methodology for optimization of the photocatalytic mineralization of CI Basic Red 46 dye from aqueous solution. *Arab. J. Chem.* **2020**, *13*, 8338–8346. [[CrossRef](#)]
26. Liu, T.; Wang, D.; Liu, H.; Zhao, W.; Wang, W.; Shao, L. Rotating packed bed as a novel disinfection contactor for the inactivation of *E. coli* by ozone. *Chemosphere* **2019**, *214*, 695–701. [[CrossRef](#)] [[PubMed](#)]
27. Qiao, J.; Luo, S.; Yang, P.; Jiao, W.; Liu, Y. Degradation of nitrobenzene-containing wastewater by ozone/persulfate oxidation process in a rotating packed bed. *J. Taiwan Inst. Chem. Eng.* **2019**, *99*, 1–8. [[CrossRef](#)]
28. Wang, L.; Yun, J.; Zhang, H.; Si, J.; Fang, X.; Shao, L. Degradation of Bisphenol A by ozonation in rotating packed bed: Effects of operational parameters and co-existing chemicals. *Chemosphere* **2021**, *274*, 129769. [[CrossRef](#)]

Disclaimer/Publisher's Note: The statements, opinions and data contained in all publications are solely those of the individual author(s) and contributor(s) and not of MDPI and/or the editor(s). MDPI and/or the editor(s) disclaim responsibility for any injury to people or property resulting from any ideas, methods, instructions or products referred to in the content.